

## IMPACT OF CELLULOSE/HYDROXYAPATITE COMPOSITES ON LIVER CELLS AND SKELETAL MUSCLE

ODETA BANIUKAITIENE,\* ALISA PALAVENIENE,\* NATALIYA BABENKO,\*\*  
VLADIMIR HARKAVENKO,\*\* VITALINA KHARCHENKO,\*\*  
ARVYDAS USAS\*\*\* and JOLANTA LIESIENE\*

\*Kaunas University of Technology, 19, Radvilenu Rd., 50254 Kaunas, Lithuania

\*\*Kharkiv V. N. Karazin National University, 4, Svobody Sq., 61022 Kharkiv, Ukraine

\*\*\*Lithuanian University of Health Sciences, 9, A. Mickeviciaus Str., 44307 Kaunas, Lithuania

✉ Corresponding author: Odetta Baniukaitiene, odeta.op@gmail.com

Received July 3, 2017

Polymer-based scaffolds with immobilised hydroxyapatite particles are among the most extensively studied materials for bone tissue regeneration. In this study, cellulose-based scaffolds with immobilised nanohydroxyapatite and microhydroxyapatite particles were prepared and analysed by micro-computed tomography. The scaffolds contained non-symmetrical interconnected pores. The porosity of the cellulose/nanohydroxyapatite and the cellulose/microhydroxyapatite scaffolds was 72% and 66%, respectively. The cytotoxicity of the cellulose-based scaffolds to hepatocytes and skeletal muscle tissue was evaluated. The results showed that the nanohydroxyapatite and the cellulose scaffolds containing nanoparticles reduced liver cell viability and increased the release of lactate dehydrogenase and aldolase. Moreover, the scaffolds containing nanohydroxyapatite particles caused cell plasma membrane damage that was manifested by significantly reduced insulin-stimulated glycogen synthesis in liver cells and glucose uptake by skeletal muscle cells. Controversially, microhydroxyapatite and the cellulose/microhydroxyapatite scaffolds had no deteriorating effect on cell survival, plasma membrane damage and glucose metabolism.

**Keywords:** nanohydroxyapatite, microhydroxyapatite, composites, cytotoxicity, hepatocytes, skeletal muscle cells

### INTRODUCTION

Polymer-based three-dimensional (3D) scaffolds are gaining considerable attention due to their potential applications for bone tissue engineering.<sup>1,2</sup> Promising results have been obtained using natural or synthetic polymers with immobilised hydroxyapatite (HA),  $\beta$ -tricalcium phosphate, bioactive glass or other inorganic particles.<sup>3-15</sup> HA is the most commonly used material for this purpose due to its similarity to the inorganic minerals of native bone tissue.<sup>16-18</sup> Moreover, HA blends with polymers can improve the mechanical stability and enhance the biointegration of the resulting composites.<sup>7,14</sup> Scaffolds that combine HA with synthetic biodegradable polymers, such as poly( $\epsilon$ -caprolactone) (PCL), poly(glycolic acid) (PGA), poly(L-lactic acid) (PLLA) and poly(D,L-lactide-co-glycolide) (PDLLGA), are among the most investigated composites in bone tissue engineering.<sup>3,6,11,13</sup>

Heo *et al.*<sup>6</sup> used PCL and HA of different particle sizes, namely nanosized (nHA, 20-90 nm) and microsized ( $\mu$ HA, 20-80  $\mu$ m) for the preparation of composite scaffolds. The scaffolds, having 72-73% porosity and a pore diameter of 500  $\mu$ m, were prepared using a modified rapid-prototyping technique. The research confirmed that the size of HA particles affected the mechanical properties of the scaffolds and cell behaviour. The compressive modulus of the nHA/PCL composite scaffolds was higher than that of the scaffolds with  $\mu$ HA. Better attachment and proliferation of human osteoblast-like cells (MG-63) was also observed on the nHA/PCL composite scaffolds.

Nejati *et al.*<sup>11</sup> synthesised rod-shaped nHA particles having 37-65 nm in width and 100-400 nm in length, and prepared nHA/PLLA composite scaffolds using the thermally

induced phase separation method. The porosity of the scaffolds was up to 85% and the pores up to 175  $\mu\text{m}$ . The prepared composites were mechanically stronger, as compared with scaffolds containing pure PLLA. Moreover, the composites were biocompatible and non-cytotoxic to mesenchymal stem cells (MSCs).

Very promising results have been obtained combining HA with naturally derived polymers, such as chitosan, alginate, starch, agarose and bacterial cellulose.<sup>5,7-10,12,15,19-22</sup> Chitosan has been mostly used for the preparation of composite scaffolds due to its high biocompatibility, biodegradability and chemical reactivity.<sup>10,12</sup> Thein-Han *et al.*<sup>20</sup> prepared highly porous chitosan/nHA scaffolds and analysed the biological response of pre-osteoblasts (MC3T3-E1) on composites and pure chitosan scaffolds. It was determined that nHA particles immobilised in the polymer improved cell attachment and proliferation, suggesting the suitability of chitosan/nHA scaffolds for bone tissue regeneration.

Zhang *et al.*<sup>22</sup> prepared chitosan-based scaffolds with nHA particles. The study showed that the presence of nHA enhanced bone tissue regeneration. The complete healing of bone defects was achieved only by using nHA/chitosan scaffolds, compared with pure chitosan.

Recently, it has been reported that the physicochemical properties of HA particles may affect the biological properties.<sup>23-25</sup> Motskin *et al.*<sup>24</sup> studied the effect of gel and colloid HA nanoparticles and microparticles on human monocyte macrophages (HMMs). The cytotoxicity was tested using the MTT assay, lactate dehydrogenase (LDH) leakage and a confocal microscopy based live-dead cell assay. The physicochemical characteristics of gel and colloid HA nanoparticles were similar, the difference was mainly in their Zeta potential. It was determined that gel and colloid nanoparticles were toxic in low concentrations, but were non-cytotoxic when using microparticles (densely packed nanoparticles). The microparticles were toxic only in high concentrations (250-500 mg/mL).

Liu *et al.*<sup>23</sup> synthesised rod-like nHA particles of different size and crystallinity *via* a hydrothermal treatment method. The researchers reported that rod-like crystals with

a diameter of approx. 23 nm, length of approx. 47 nm and crystallinity of 85% gave a better biological response in promoting MG-63 osteoblasts growth and inhibiting cell apoptosis, in comparison with smaller crystals. It was found that rod-like crystals with a diameter of approx. 16 nm, a length of approx. 40 nm and crystallinity of 65% can trigger an inflammatory response. Controversially, Shi *et al.*<sup>25</sup> determined that spherical nHA particles with a diameter of 20 nm exhibited better effects than those with a diameter of 80 nm by promoting MG-63 cell growth and inhibiting cell apoptosis. Zhao *et al.*<sup>26</sup> studied the influence of the morphology of HA nanoparticles on cytotoxicity to BEAS-2B (human bronchial epithelial cells) and RAW264.7 (murine macrophages). They used nHA of different shapes, namely needles (nHA-ND), plates (nHA-PL), spheres (nHA-SP) and rods (nHA-RD). The results showed that nHA-PL and nHA-ND induced the highest cytotoxicity to BEAS-2B cultures, compared with those of nHA-RD or nHA-SP. However, no significant toxicity was observed in RAW264.7 cultures exposed to any of the nHA groups.

A concise literature review indicates that there is a lack of understanding about the biocompatibility of HA and the polymeric composites with HA because controversial results have been reported. It could be only assumed that the biological properties of HA depend on the size and morphology of the particles, physicochemical properties and concentration. The results of the cytotoxicity studies also depend on the cell type used for the studies. Moreover, no studies comparing the cytotoxicity of HA particles immobilised in a polymeric network with that of pure HA particles were found. Therefore, no unambiguous conclusions on the biological properties of HA particles and polymer/HA composites can be made.

The aim of this study is to prepare 3D scaffolds of regenerated cellulose with immobilised nano- and microhydroxyapatite particles and to evaluate the potential toxicity and biocompatibility of the composite scaffolds using liver cells and skeletal muscle tissue.

## EXPERIMENTAL

### Preparation of cellulose/hydroxyapatite composites

Cellulose scaffolds with immobilised hydroxyapatite (HA) particles were prepared by mechanically inserting nanohydroxyapatite (nHA, average particle size of 100 nm, Sigma-Aldrich Co., USA) or microhydroxyapatite ( $\mu$ HA, average particle size of 20  $\mu$ m, Sigma-Aldrich Co., USA) spherical particles during the formation of a cellulose gel from cellulose acetate (Sigma-Aldrich Co., USA, degree of substitution 2.4).<sup>4</sup> Composites were formulated with HA particles of 50 wt% and dried using the freeze-drying technique (Christ ALPHA 2-4 LSC freeze dryer, Martin Christ Gefriertrocknungsanlagen GmbH, Germany).<sup>27</sup>

### Micro-computed tomography

The micro-computed tomography (micro-CT) analysis was performed using a  $\mu$ CT40 system (Scanco Medical AG, Switzerland). A sample of the scaffold in the form of a cylinder with a diameter of 10 mm and a height of 8 mm was used for the analysis. The following parameters were used for the scans: energy, 45 kVp; integration time, 600 ms; scanning medium, air; frame averaging, 2x; and nominal resolution, 10  $\mu$ m. The data were filtered using a constrained 3D Gaussian filter to partially suppress the noise in the images ( $\sigma=0.8$ , support=1). Two-dimensional (2D) and 3D images were generated using image reconstruction software provided by the manufacturer. Scanco evaluation software was used for the quantitative evaluation of structural parameters of the scaffolds.

### Cytotoxicity tests

#### Cell viability

The effect of the scaffolds on cell viability was analysed by using hepatocytes isolated from the liver of 3-month-old Wistar rats.<sup>28</sup> Immediately after isolation, cell aliquots were stained with trypan blue dye and counted using a haemocytometer. The viability of the isolated hepatocytes before incubation in all the experiments was greater than 95%. The initial cell batch isolated from rat liver was constituted of  $1.5 \times 10^9$  cells in 15 mL, and after counting and vital staining with trypan blue consequently diluted down to  $2 \times 10^7$  cells/mL. After isolation, the cells were incubated in Petri dishes at 37 °C, saturated (99%) humidity and 5% CO<sub>2</sub> for 90 min with composite samples or HA powders at 50 mg/mL and 10 mg/mL of cell suspension, respectively. After incubation, aliquots were collected for cell count and viability testing. Cell viability was determined by staining with trypan blue dye.  $\geq 600$  cells for every sample group in the set of experiments were tested. Control cell viability was

greater than 92%, in all the experiments.

### LDH and aldolase release

The integrity of the cell plasma membrane was tested on isolated rat hepatocytes and *extensor digitorum longus* (EDL) muscle tissue by evaluating LDH and aldolase activity, respectively. LDH and aldolase release from the cells indicates membrane damage.<sup>29,30</sup> In order to evaluate hepatocyte membrane damage, cells were centrifuged after incubation with the composites, and supernatants were collected for LDH assay. LDH release into the supernatant was detected using a commercially available kit (LDH UV SCE) from Felecity Diagnostic (Dnepropetrovsk, Ukraine). To investigate potential membrane damage in myocytes, EDL muscle tissue was isolated from 3-month-old Wistar rats and incubated with the composite samples at 37 °C for 90 min in an oxygen-enriched Krebs saline buffer. Incubation medium was used for the aldolase assay.<sup>31</sup>

### Insulin-induced glycogen synthesis and glucose uptake

The metabolic effects of the cellulose/HA composites were studied in isolated hepatocytes and EDL muscle tissue by evaluating liver and muscle tissue sensitivity to insulin after 90 min incubation with the samples. Isolated hepatocytes were used to determine insulin-induced glycogen synthesis by the method of Brutman-Barazani *et al.*<sup>32</sup>

Cells were washed in the HBS buffer (HEPES-buffered saline) containing 20 mM HEPES. To determine glycogen synthesis, the hepatocytes were incubated in HBS buffer in the presence of 5 mM glucose, 10 nM insulin or 0.9% NaCl (control), and 0.1  $\mu$ Ci/mL of D-[U<sup>14</sup>C] glucose for 2 h at 37 °C. The reaction was stopped with ice-cold 0.9% NaCl and the hepatocytes were washed with the same solution three times. The cells were lysed with 50 mM NaOH. To analyse the insulin-induced glucose uptake by the skeletal muscle tissue, 2-D-[<sup>3</sup>H] glucose (0.5  $\mu$ Ci/mL) and isolated EDL muscles were used. The radioactivity of the newly synthesised <sup>14</sup>C-glycogen and <sup>3</sup>H-glucose was measured by using a BETA scintillation counter.

### Statistical analysis

The results of cytotoxicity were expressed as a mean  $\pm$  standard deviation of five independent experiments. One-way analysis of variance (ANOVA) procedures was used to assess significant differences among the treatment groups. The student's t-test was used for paired observations.

## RESULTS AND DISCUSSION

### Characterisation of cellulose-based scaffolds

In our study, the cytotoxicity of 3D cellulose composites with HA particles was examined. Spherical HA particles of two different sizes, namely nHA (average particle size of 100 nm) and  $\mu$ HA (average particle size of 20  $\mu$ m) were used. The morphological parameters of the scaffolds were examined by micro-CT. 2D images showed that the size of HA particles had a major impact on scaffold morphology. There were clear differences in pore size, framework thickness and distribution between different scaffold groups (Fig. 1, Table 1). The scaffolds contained non-symmetrical interconnected pores. Such arrangement of the pores is particularly important for cellular activity and supports the optimal rate of the new tissue growth. The structural parameters of the scaffolds, such as the percent framework volume ( $X_v$ ), the porosity ( $P$ ), the specific scaffold surface area ( $SS$ ), mean framework thickness ( $L$ ) and mean pore diameter ( $D$ ), which are summarised in Table 1, were determined from 3D images (Figure 1b, d). The quantitative analysis showed that the porosity of the cellulose/nHA scaffold was larger, leading to a reduced percentage of the framework volume, as

compared with the cellulose/ $\mu$ HA scaffold. The frameworks of the cellulose/ $\mu$ HA scaffold were almost twice thicker, in comparison with the frameworks of the cellulose/nHA. The specific surface area of cellulose/nHA was larger due to the thinner frameworks and their higher number per millimeter. The cellulose/nHA scaffold had smaller pores (490  $\mu$ m and 540  $\mu$ m of the cellulose/nHA and cellulose/ $\mu$ HA scaffold, respectively) (Table 1). These values correlated well with the required ones ( $\geq 100 \mu$ m).<sup>2</sup>

We assume that HA particle size could influence the homogeneity of the prepared cellulose/HA blends. nHA resulted in more uniform distribution of particles within the solution. Our findings agree with the results of Mi *et al.*<sup>33</sup> Oppositely,  $\mu$ HA particles were probably influenced by gravitational forces and therefore sedimentation and/or agglomeration of a certain amount of particles occurred.<sup>34</sup> As a result, the expanded solution within the cellulose/ $\mu$ HA scaffold formed large pores and thick frameworks. On the contrary, nHA distributed well within the cellulose/nHA scaffold, leading to the formation of smaller pores and thinner frameworks. Despite the differences, both composites displayed structural parameters that mimic the structure of a native bone.<sup>35</sup>

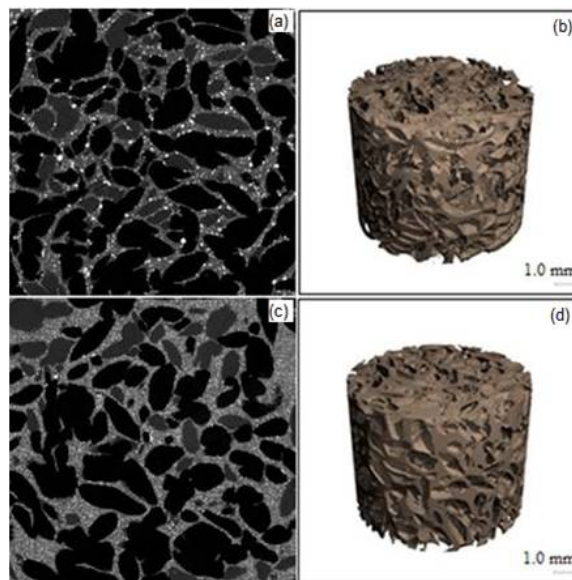


Figure 1: 2D and 3D micro-CT images: (A, B) cellulose/nHA scaffold and (C, D) cellulose/ $\mu$ HA scaffold

Table 1  
Structural parameters of the scaffolds

Scaffold type	Structural parameters				
	X <sub>v</sub> (%)	P (%)	SS (mm <sup>-1</sup> )	L (mm)	D (mm)
Cellulose/nHA	28 ± 0.94	72 ± 1.72	19 ± 0.25	0.12 ± 0.01	0.49 ± 0.09
Cellulose/μHA	34 ± 1.11	66 ± 2.09	13 ± 0.50	0.21 ± 0.01	0.54 ± 0.13

### Biocompatibility and cytotoxicity of the scaffolds

Cellulose is known as a biocompatible non-cytotoxic polymer. Concerning HA, contradictory reports on its cytotoxicity and the effect of its particle size on cell viability are found.<sup>36-38</sup> The majority of scientists declare that nanosized HA may cause cytotoxicity. Furthermore, Wang *et al.*<sup>39</sup> analysed the biological data about engineered HA used in bone repair and clarified the adverse biological effect of nanosized HA. However, there is no scientific data on the cytocompatibility of HA particles immobilised in a polymeric matrix. We expected that immobilisation should reduce the cytotoxic effect of nanosized particles on the cells.

With the aim to ascertain the effect of immobilised HA particles on the cells, the cellulose-based scaffolds with nHA and μHA particles were examined. The nanosized and microsized HA particles alone, as well as the cellulose matrix without HA, were studied for comparison. Liver cells and skeletal muscle tissue were used for these studies due to their high sensitivity. Moreover, hepatocytes are the most commonly used for assessment of new pharmaceutical drugs. Several

hepatocyte-based toxicological models are available. Cultures of primary hepatocytes are still considered to be the gold standard *in vitro* model system.<sup>40</sup>

The biocompatibility and cytotoxicity of the cellulose/HA scaffolds were evaluated by testing cell viability, plasma membrane integrity and metabolic effects on hepatocytes and EDL muscle tissue.

### Hepatocyte viability

Hepatocyte viability was studied by incubation of the scaffolds and HA particles with the cells isolated from the liver of rats. Freshly isolated hepatocytes, cultured under the same conditions as the experimental groups, were assigned as the control group. The cellulose scaffolds and scaffolds containing μHA particles demonstrated negligible changes in hepatocyte viability (Fig. 2). However, the cellulose/nHA scaffolds reduced the viability of cells, in comparison with the control. Furthermore, hepatocyte incubation with HA powders demonstrated that μHA particles had no significant effect on cell viability.

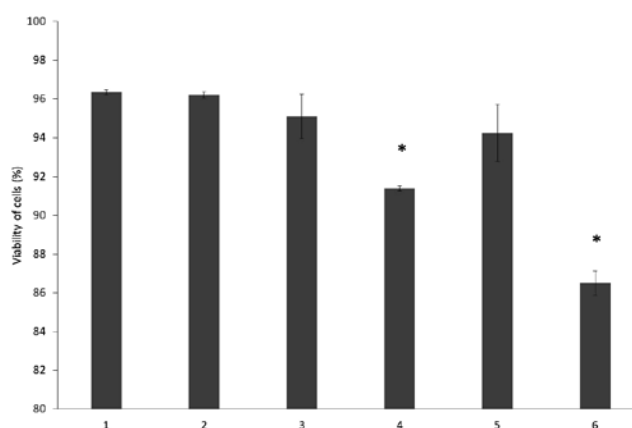


Figure 2: Effect of cellulose scaffold, cellulose/HA composite scaffolds and HA powdered particles on hepatocyte viability: 1 – control cells, 2 – cellulose scaffold, 3 – cellulose/μHA, 4 – cellulose/nHA, 5 – μHA particles, 6 – nHA particles; \*p<0.05

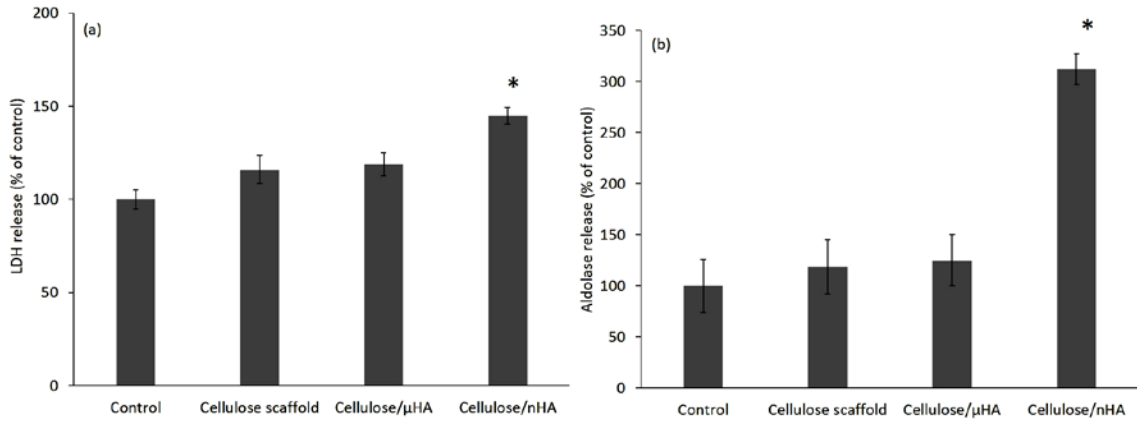


Figure 3: Effect of cellulose scaffold and cellulose/HA composite scaffolds on LDH and aldolase release into the incubation medium: (A) LDH release from hepatocytes and (B) aldolase release from EDLs; \*p<0.05

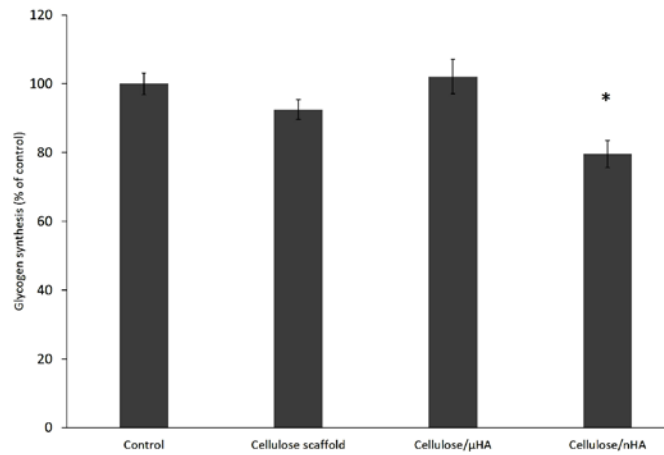


Figure 4: Effect of cellulose scaffold and cellulose/HA composite scaffolds on glycogen synthesis in hepatocytes; \*p<0.05

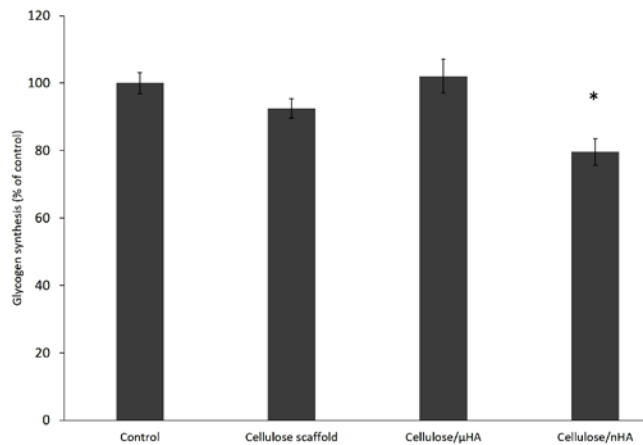


Figure 5: Effect of cellulose scaffold and cellulose/HA composite scaffolds on insulin-induced glucose uptake in EDL muscles; \*p<0.05

At the same time, nHA powder significantly reduced cell viability (Fig. 2). Nevertheless, it should be noted that, when nHA particles were immobilised in the

cellulose matrix, the cytotoxic effect was reduced.

**Cell membrane damage**

Further, to evaluate the damaging effects of

the cellulose/HA scaffolds on cell membrane integrity, the release of cellular enzymes, namely LDH and aldolase, into the incubation media was investigated. Having pre-incubated hepatocytes with the cellulose/nHA scaffolds, a significant increase in LDH activity in the incubation medium was detected. In contrast, the cellulose scaffolds and the cellulose/ $\mu$ HA composites had no significant LDH release from the cells, with regard to the control group (Fig. 3a). When incubated with EDL tissue, the cellulose/nHA scaffolds also significantly amplified aldolase activity in the culture medium – an approximately 3-fold increase was noted compared to the control (Fig. 3b). At the same time, the cellulose scaffolds without HA and with  $\mu$ HA did not change the aldolase release from the cells (Fig. 3b). The enzymatic activity, elevated in the incubation medium of hepatocytes and muscle tissue after pre-incubation with the scaffolds, containing nHA particles, indicates membrane damage caused by the composite. This may lead to metabolic dysregulation and cell death.

### **Metabolic effects**

Liver cells and skeletal muscle are classical target tissues for insulin action. Glucose metabolism is under insulin control. Reduced cell sensitivity to insulin action is a common feature of metabolic syndrome and type 2 diabetes. Reduced cell viability is followed by reduced insulin stimulation of glucose uptake and glycogen synthesis.<sup>28</sup>

Significant insulin-induced [<sup>14</sup>C] glycogen synthesis failure was found in the cells incubated with the cellulose/nHA scaffolds, in comparison with the isolated EDL slice (the control group) (Fig. 4). The cellulose/nHA scaffolds decreased the [<sup>14</sup>C] glycogen synthesis rate in the insulin-treated cells by approximately 20%, compared to the control, while the whole-cellulose scaffolds and the cellulose/ $\mu$ HA composites did not affect the [<sup>14</sup>C] glycogen synthesis rate in the hepatocytes. At the same time, the scaffolds containing nHA induced a 2-fold [<sup>3</sup>H] glucose uptake in the insulin-stimulated EDL cells, in comparison with the control, while the other composite scaffolds caused no significant changes in the [<sup>3</sup>H] glucose uptake rate (Fig. 5).

The observed results ensure that nHA and

the scaffolds containing nanoparticles markedly reduce insulin-stimulated glycogen synthesis in the liver cells and glucose uptake by muscle cells. These results coincide with those reported by other scientists.<sup>24,26</sup> However, the cytotoxic effect was reduced when the particles were immobilised in the polymer. To the best of our knowledge, no previous reports in the literature exist regarding this matter.

### **CONCLUSION**

The biocompatibility and potential toxicity of nanohydroxyapatite and microhydroxyapatite and their composite scaffolds with cellulose were tested by means of three different methods, such as hepatocyte viability, cell membrane integrity and response to insulin. The cellulose/nanohydroxyapatite scaffolds revealed slight cytotoxicity and down regulated insulin sensitivity in hepatocytes and *extensor digitorum longus* muscle tissue. Moreover, the nanohydroxyapatite particles alone demonstrated cytotoxic effects, compared to the control sample and to microhydroxyapatite particles. Simultaneously, the cellulose composites with microhydroxyapatite particles demonstrated acceptable levels of cell integrity and viability during the incubation period and showed no cytotoxic or damaging effect on primarily isolated liver cells and skeletal muscle.

**ACKNOWLEDGMENT:** The authors are grateful to the Lithuanian Research Council for financial support (grants MIP019/2014 and TAP LU 01/2014) and the State Agency for Science, Innovation and Informatization of Ukraine (grant M/127-2014).

### **REFERENCES**

- <sup>1</sup> N. Ninan, Y. Grohens, A. Elain, N. Kalarikkal and S. Thomas, *Eur. Polym. J.*, **49**, 2433 (2013).
- <sup>2</sup> V. Karageorgiou and D. Kaplan, *Biomaterials*, **26**, 5476 (2005).
- <sup>3</sup> N. Aboudzadeh, M. Imani, M. A. Shokrgozar, A. Khavandi, J. Javadpour *et al.*, *J. Biomed. Mater. Res.*, **94**, 137 (2010).
- <sup>4</sup> O. Petrauskaitė, P. S. Gomes, M. H. Fernandes, G. Juodzbalytė, A. Stumbras *et al.*, *Biomed. Res. Int.*, **2013**, 1 (2013).
- <sup>5</sup> B. M. Chesnutt, A. M. Viano, Y. Yuan, Y. Yang, T. Guda *et al.*, *J. Biomed. Mater. Res. A.*, **88**,

491 (2009).

<sup>6</sup> S. Heo, S. Kim, J. Wei, Y. Hyun, H. Yun *et al.*, *J. Biomed. Mater. Res. A.*, **89**, 108 (2009).

<sup>7</sup> A. K. Bajpai and H. Bundela, *Compos. Interface*, **15**, 709 (2008).

<sup>8</sup> Q. Hu, B. Li, M. Wang and J. Shen, *Biomaterials*, **25**, 779 (2004).

<sup>9</sup> J. Liuyun, L. Yubao and X. Chengdong, *J. Mater. Sci. - Mater. Med.*, **20**, 1645 (2009).

<sup>10</sup> F. Akman, *Cellulose Chem. Technol.*, **51**, 253 (2017).

<sup>11</sup> E. Nejati, H. Mirzadeh and M. Zandi, *Compos. A, Appl. Sci. Manuf.*, **39**, 1589 (2008).

<sup>12</sup> Z. Moridi, V. Mottaghitalab and A. K. Haghi, *Cellulose Chem. Technol.*, **45**, 549 (2011).

<sup>13</sup> V. Thomas, S. Jagani, K. Johnson, M. V. Jose, D. R. Dean *et al.*, *J. Nanosci. Nanotechnol.*, **6**, 487 (2006).

<sup>14</sup> C. P. Tsui, C. Y. Tang, Y. Q. Guo, P. S. Uskokovic, I. P. Fan *et al.*, *Compos. Interface*, **17**, 571 (2010).

<sup>15</sup> J. Zhang, J. Nie, Q. Zhang, Y. Li, Z. Wang *et al.*, *J. Biomater. Sci. Polym. Ed.*, **25**, 61 (2014).

<sup>16</sup> S. V. Dorozhkin, *J. Mater. Sci.*, **42**, 1061 (2007).

<sup>17</sup> L. C. Palmer, C. J. Newcomb, S. R. Kaltz, E. D. Spoerke and S. I. Stupp, *Chem. Rev.*, **108**, 4754 (2008).

<sup>18</sup> J. Corona-Gomez, X. Chen and Q. Yang, *J. Funct. Biomater.*, **7**, 18 (2016).

<sup>19</sup> K. Madhumathi, K. Shalumon, V. V. Rani, H. Tamura, T. Furuike *et al.*, *Int. J. Biol. Macromol.*, **45**, 12 (2009).

<sup>20</sup> W. W. Thein-Han and R. D. K. Misra, *Acta Biomater.*, **5**, 1182 (2009).

<sup>21</sup> J. Venkatesan and S. Kim, *Mar. Drugs*, **8**, 2252 (2010).

<sup>22</sup> X. Zhang, L. Zhu, H. Lv, Y. Cao, Y. Liu *et al.*, *J. Mater. Sci. - Mater. Med.*, **23**, 1941 (2012).

<sup>23</sup> X. Liu, M. Zhao, J. Lu, J. Ma, J. Wei *et al.*, *Int. J. Nanomed.*, **7**, 1239 (2012).

<sup>24</sup> M. Motskin, D. Wright, K. Muller, N. Kyle, T. G. Gard *et al.*, *Biomaterials*, **30**, 3307 (2009).

<sup>25</sup> Z. Shi, X. Huang, Y. Cai, R. Tang and D. Yang, *Acta Biomater.*, **5**, 338 (2009).

<sup>26</sup> X. Zhao, S. Ng, B. C. Heng, J. Guo, L. Ma *et al.*, *Arch. Toxicol.*, **87**, 1037 (2013).

<sup>27</sup> O. Petrauskaite, G. Juodzbaly, P. Viskelis and J. Liesiene, *Cellulose Chem. Technol.*, **50**, 23 (2016).

<sup>28</sup> N. Babenko and V. Kharchenko, *Biochemistry*, **77**, 180 (2012).

<sup>29</sup> N. A. Babenko and E. G. Shakhova, *Lipids Health Dis.*, **7**, 1 (2008).

<sup>30</sup> Y. Hathout, R. L. Marathi, S. Rayavarapu, A. Zhang, K. J. Brown *et al.*, *Hum. Mol. Genet.*, **23**, 6458 (2014).

<sup>31</sup> N. Swetha, *RRJZS*, **S2**, 101 (2016).

<sup>32</sup> T. Brutman-Barazani, M. Horovitz-Fried, S. Aga-Mizrachi, C. Brand, C. Brodie *et al.*, *J. Cell. Biochem.*, **113**, 2064 (2012).

<sup>33</sup> H. Y. Mi, S. Palumbo, X. Jing, L. S. Turng, W. J. Li *et al.*, *J. Biomed. Mater. Res. B Appl. Biomater.*, **102**, 1434 (2014).

<sup>34</sup> W. Abdelwahed, G. Degobert, S. Stainmesse and H. Fessi, *Adv. Drug Deliv. Rev.*, **58**, 1688 (2006).

<sup>35</sup> J. Kim, J. Shin, S. Oh, W. Yi, M. Heo *et al.*, *Imaging Sci. Dent.*, **43**, 227 (2013).

<sup>36</sup> X. Zhao, B. C. Heng, S. Xiong, J. Guo, T. T. Tan *et al.*, *Nanotoxicology*, **5**, 182 (2011).

<sup>37</sup> R. Lima, A. B. Seabra and N. Durán, *J. Appl. Toxicol.*, **32**, 867 (2012).

<sup>38</sup> K. B. Ramadi, Y. A. Mohamed, A. Al-Sbiei, S. Almarzooqi, G. Bashir *et al.*, *Nanotoxicology*, **10**, 1061 (2016).

<sup>39</sup> J. Wang, L. Wang and Y. Fan, *Int. Mol. Sci.*, **17**, 798 (2016).

<sup>40</sup> V. Y. Soldatow, E. L. LeCluyse, L. G. Griffith and I. Rusyn, *Toxicol. Res. (Camb.)*, **2**, 23 (2013).